Attribution of Lake Surface Water Temperature Change in Large Lakes Across China Over Past Four Decades

Ling Huang, Xuhui Wang, Yanzi Yan, Lei Jin, Kun Yang, Anping Chen, Rongshun Zheng, Catherine Ottle, Chenzhi Wang, Yaokui Cui, et al.

▶ **To cite this version:**

Ling Huang, Xuhui Wang, Yanzi Yan, Lei Jin, Kun Yang, et al.. Attribution of Lake Surface Water Temperature Change in Large Lakes Across China Over Past Four Decades. Journal of Geophysical Research: Atmospheres, 2023, 128 (21), pp.e2022JD038465. 10.1029/2022JD038465 . hal-04275224

HAL Id: hal-04275224
https://hal.science/hal-04275224v1

Submitted on 9 Jan 2025

HAL is a multi-disciplinary open access archive for the deposit and dissemination of scientific research documents, whether they are published or not. The documents may come from teaching and research institutions in France or abroad, or from public or private research centers.

L'archive ouverte pluridisciplinaire **HAL**, est destinée au dépôt et à la diffusion de documents scientifiques de niveau recherche, publiés ou non, émanant des établissements d'enseignement et de recherche français ou étrangers, des laboratoires publics ou privés.

Copyright

Check for updates

JGR Atmospheres

RESEARCH ARTICLE
10.1029/2022JD038465

Special Section:
Land-atmosphere coupling: measurement, modelling and analysis

Attribution of Lake Surface Water Temperature Change in Large Lakes Across China Over Past Four Decades

Ling Huang[1], Xuhui Wang[1], Yanzi Yan[1], Lei Jin[1], Kun Yang[2], Anping Chen[3], Rongshun Zheng[1], Catherine Ottlé[4], Chenzhi Wang[1,5], Yaokui Cui[6], and Shilong Piao[1]

[1]College of Urban and Environmental Sciences, Sino-French Institute for Earth System Science, Peking University, Beijing, China, [2]Department of Earth System Science, Ministry of Education Key Laboratory for Earth System Modeling, Institute for Global Change Studies, Tsinghua University, Beijing, China, [3]Department of Biology, Colorado State University, Fort Collins, CO, USA, [4]Laboratoire des Sciences du Climat et de l'Environnement, IPSL, CNRS-CEA-UVSQ, Gif-sur-Yvette, France, [5]Leibniz Centre for Agricultural Landscape Research (ZALF), Müncheberg, Germany, [6]School of Earth and Space Sciences, Institute of RS and GIS, Peking University, Beijing, China

Key Points:

- Lake model revealed a significant annual increase of 0.040°C ($p < 0.05$) in the surface water temperature of large lakes across China from 1979 to 2018
- The simulated surface water temperature warmed faster than the local surface air temperature in approximately 42% of the studied lakes
- Changes in air temperature, downward longwave radiation, and wind speed are the primary contributors to the trends in lake surface water temperature

Supporting Information:

Supporting Information may be found in the online version of this article.

Correspondence to:

X. Wang,
xuhui.wang@pku.edu.cn

Citation:

Huang, L., Wang, X., Yan, Y., Jin, L., Yang, K., Chen, A., et al. (2023). Attribution of lake surface water temperature change in large lakes across China over past four decades. *Journal of Geophysical Research: Atmospheres*, *128*, e2022JD038465. https://doi.org/10.1029/2022JD038465

Received 30 DEC 2022
Accepted 22 OCT 2023

© 2023. American Geophysical Union. All Rights Reserved.

Abstract Lake surface water temperature (LSWT) is a key parameter in lake energy budget and is highly vulnerable to climate change. However, the long-term trends in LSWT across China and their driving factors remain uncertain. Here, we used a calibrated lake model to simulate LSWT over 1979–2018 for 91 large lakes (>100 km^2) across China. Simulations reveal an overall LSWT warming trend (0.040°C yr^{-1}, $p < 0.05$), but with large spatial variations. The majority of these lakes show significant warming trends (84%, 0.053°C yr^{-1}), while a significant cooling trend is found in the seven lakes in the northwestern Tibetan Plateau (−0.064°C yr^{-1}). LSWT of approximately 42% of the lakes increases more rapidly than the corresponding ambient air temperature. Regionally, the warming trend is highest for lakes in the Eastern Plain (0.049°C yr^{-1}) and the lowest in the Yunnan-Guizhou Plateau (0.016°C yr^{-1}). The increases in simulated LSWT also vary across seasons, with a higher rate in winter and spring than in summer and autumn. Changes in air temperature, downward longwave radiation, and wind speed are the most important climatic drivers for LSWT changes. Lake surface warming could be more rapid under future global warming, necessitating greater attention to lake-atmosphere interactions.

Plain Language Summary Lake surface water temperature (LSWT) is an essential factor in regulating heat and water exchange between lake surface and air. Previous studies have relied on satellite or in situ data to study changes in LSWT at various scales. However, the spatiotemporal variations in LSWT at a national scale and their driving factors are still poorly understood for large countries such as China. Here, we used a one-dimensional lake model (FLake) to simulate the spatiotemporal variability of LSWT for 91 large lakes (>100 km^2) across China from 1979 to 2018. Our simulations reveal a significant warming trend for most lakes, although a few lakes in the northwestern Tibetan Plateau show a cooling trend. Interestingly, 42% (38 of 91) of these lakes showed faster warming rates than nearby air temperatures. LSWT increased faster in spring and winter than in summer and autumn. Lake surface warming is mainly explained by locally rising air temperature, increasing downward longwave radiation, and weakened wind speed. Under the projected warmer climate in the future, lake surface warming is expected to continue, with important implications for lake management and climate change mitigation.

1. Introduction

Lakes are important moisture sources for the lower atmosphere (Wang et al., 2019). Lake surface water temperature (LSWT) affects the energy and mass exchange between the lake surface and the atmosphere, which modulates the weather and climate at local to regional scales (Steiner et al., 2013). Moreover, LSWT plays a critical role in regulating the physical and biogeochemical processes of lake ecosystems (Adrian et al., 2009). Changes in LSWT can substantially impact the functioning of lake ecosystems and, sometimes, even that of terrestrial ecosystems through the coupling of land-aquatic ecosystems. Rising LSWT could strengthen thermal stability (Kraemer et al., 2015), weaken vertical exchange of oxygen (O'Reilly et al., 2003), increase cyanobacteria growth (Paerl & Paul, 2012), and further deteriorate water quality (Paerl & Huisman, 2008). With climate warming over the past decades, LSWT is among the first state variables of lakes responding to climate change and is expected to increase (O'Reilly et al., 2015; Woolway et al., 2017). However, it remains largely elusive on how fast does LSWT

21698996, 2023, 21, Downloaded from https://agupubs.onlinelibrary.wiley.com/doi/10.1029/2022JD038465 by Portail BibCNRS INSU, Wiley Online Library on [09/01/2025]. See the Terms and Conditions (https://onlinelibrary.wiley.com/terms-and-conditions) on Wiley Online Library for rules of use; OA articles are governed by the applicable Creative Commons License

change in response to climate change across different regions and lake types and what determines the spatiotemporal variation in LSWT changes. Addressing these questions is important for understanding the impacts of climate change on both lake and its surroundings.

Based on lake surface energy budgets, Schmid et al. (2014) estimated that the increase in equilibrium LSWT should equate to 70%–85% of the rise in air temperature at the global scale, assuming no changes in other forcing variables. However, processes driving lake warming could be much more complex at a finer scale. For example, decreased ice cover (Austin & Colman, 2007), increased solar radiation (Li et al., 2019; Zhong et al., 2016), earlier lake stratification (Woolway & Merchant, 2017), and water clarity change (Heiskanen et al., 2015) could further accelerate lake warming, even leading to higher LSWT warming than the air warming under certain specific circumstances (Austin & Colman, 2007; O'Reilly et al., 2015; Schmid & Köster, 2016). Although changes in LSWT have been studied at various scales worldwide, the spatiotemporal pattern of LSWTs responding to climate change at a national scale in China has not been analyzed yet.

Here, we aim to quantify LSWT changes for large lakes in China over the past four decades. As of 2015, China had 2,756 natural lakes with an area greater than 1.0 km^2, covering 1% of its land area in total (Tao et al., 2019). These lakes occur in regions with distinct climatic and hydrological characteristics (Ma et al., 2011). Previous research, however, focused on LSWT of an individual lake or a specific region, for example, large lakes in the Tibetan Plateau (TP) (Shi et al., 2022; Wan et al., 2018; Zhang et al., 2014), Yunnan-Guizhou Plateau (YG) (Yang et al., 2019), or the Yangtze River Basin (Li et al., 2019). These studies revealed large differences in the LSWT trends among certain regions. A wide range of the warming trends of LSWT from 0.012°C yr^{-1} (Zhang et al., 2014) to 0.042°C yr^{-1} (Yang et al., 2020) has been reported for the TP and YG during the past 20 years. Even within the same region, different satellite products with varying periods of observation could show diverging trends of LSWT (Shi et al., 2022). Therefore, a national-scale estimate of long-term LSWT trends with consistent methods is clearly needed.

Lake models are an essential tool in understanding long-term temporal variations of LSWT (L. Huang et al., 2021; Layden et al., 2016; Li et al., 2019) and are capable of separating contributions of individual climatic factors to LSWT changes. Here, we used a calibrated one-dimensional lake model FLake (freshwater lake model) to simulate the spatiotemporal variations of LSWT for 91 large lakes (>100 km^2) in China and quantify the relative contributions of climatic factors to LSWT trends over the past four decades (1979–2018). In our study, LSWT refers to the surface temperature of lakes, including both water surface temperature and ice surface temperature. Specifically, we first evaluated FLake model simulations against satellite-derived LSWT data. Then, we investigated the spatiotemporal pattern of modeled LSWT at the sub-region scale. Finally, we performed factorial experiments to calculate the relative contributions of different climatic factors to LSWT changes. Our integrated method with both satellite data and model simulations offers a reliable approach for detecting and attributing LSWT changes for large lakes in China.

2. Materials and Methods

2.1. Criteria of Lake Selection

We extracted 112 large lakes in China with an area greater than 100 km^2 from the HydroLAKES data set (Messager et al., 2016). The FLake model was developed to simulate the thermal changes in freshwater lakes, so we excluded hyper-saline lakes based on the China Salty Lakes Resources and Environment Database (http://yhzyhj.isl.ac.cn/). However, brackish lakes were not excluded since the FLake model can reasonably simulate temperature changes in such lakes, like Qinghai Lake and Namco Lake (A. N. Huang et al., 2019; Su et al., 2019). Moreover, two large lakes in the Inner-Mongolia Plateau that have disappeared over the past few decades due to drought and human activities were not simulated (Tao et al., 2015). Ultimately, we conducted our study on water temperature changes in 91 large lakes, which represent approximately half of the Chinese total lake area (Figure 1). These lakes are heterogeneous regarding their morphological, climatic, and geographical conditions. We categorized them into six sub-regions according to their geographical and climatic features (Ma et al., 2011). These sub-regions include the TP (53 lakes), Xinjiang (XJ, 6 lakes), Inner-Mongolia Plateau (MP, 3 lakes), Northeast Plain and Mountain (NE, 4 lakes), Eastern Plain (EP, 22 lakes), and YG (3 lakes).

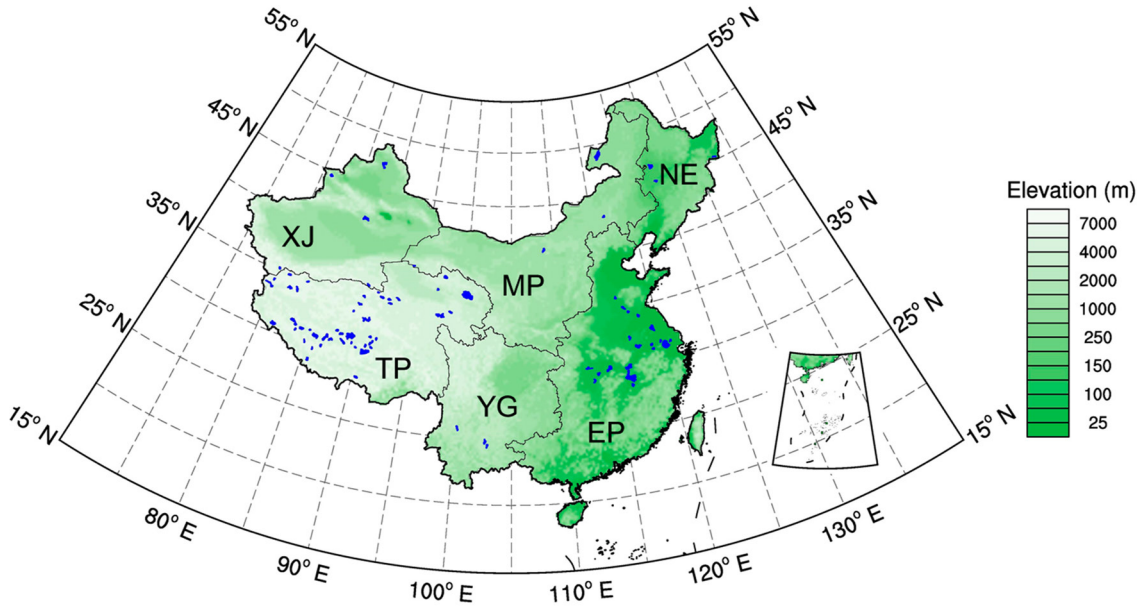

Figure 1. Locations of the studied lakes (blue areas) in China. The six sub-regions include the Tibetan Plateau (TP), Xinjiang (XJ), Inner-Mongolia Plateau (MP), Northeast Plain and Mountain (NE), Eastern Plain (EP), and Yunnan-Guizhou Plateau (YG). The green rendered map indicates the elevation obtained from Shuttle Radar Topography Mission Digital Elevation Database v4.1. The inset map shows the Nanhai Zhudao.

2.2. Data

2.2.1. Lake Data

Information on the geomorphic characteristics of different lakes (lake boundary and lake area) is acquired from the HydroLAKES data set (Messager et al., 2016). To simulate individual lakes accurately, lake-specific parameters were required for each lake, including effective lake depth, light extinction coefficient, water albedo, white ice albedo, blue ice albedo, and fetch. L. Huang et al. (2021) estimated these lake-specific parameters to closely reproduce the observed surface temperature dynamics, with a specific focus on minimizing the root-mean-square error (RMSE) between FLake output and ARC-Lake (ATSR Reprocessing for Climate: LSWT & Ice Cover) surface water temperatures. These lake-specific parameters significantly improved the simulation capability of FLake in China. Of the 91 selected lakes, 85 lakes had available lake-specific parameters from L. Huang et al. (2021) to force the FLake model. The remaining six lakes were simulated using lake-specific parameters from the geographically nearest available lakes.

2.2.2. Forcing Data

China Meteorological Forcing Dataset (CMFD), with a spatial resolution of 0.1° and temporal resolution of 3 hr from 1979 to 2018, was used to drive the FLake model (He et al., 2020). This data set assimilating remote sensing products, climate reanalysis data, and meteorological observation data, has been widely used in studies of land surface processes and hydrological modeling in China (Lazhu et al., 2016; Wang et al., 2019). The long-term trends of individual forcing variables in the CMFD data set are consistent with those observed in situ (Guo & Wang, 2013; Peng et al., 2021; Yang et al., 2021). For each lake, the forcing data, for example, air temperature, wind speed, downward radiation, etc., are spatially averaged over the lake to minimize the effect of intralake heterogeneity. More information about the forcing variables will be explained in Section 2.3. The wind speed provided in the CMFD was based on wind speed measurements over lands where wind speed is weaker than that of large lakes. As a result, the CMFD data set may not accurately represent the wind speed over large lakes. The scaling of wind speed equation (Equation 1) proposed by Hsu (1988) was used to correct the bias.

$$U_{\text{lake}} = 1.62 + 1.17 \times U_{\text{land}} \quad (1)$$

In Equation 1, U_{lake} is the wind speed over lake (m s^{-1}), and U_{land} is the wind speed over land (m s^{-1}).

21698996, 2023, 21, Downloaded from https://agupubs.onlinelibrary.wiley.com/doi/10.1029/2022JD038465 by Portail BibCNRS INSU, Wiley Online Library on [09/01/2025]. See the Terms and Conditions (https://onlinelibrary.wiley.com/terms-and-conditions) on Wiley Online Library for rules of use; OA articles are governed by the applicable Creative Commons License

21698996, 2023, 21, Downloaded from https://agupubs.onlinelibrary.wiley.com/doi/10.1029/2022JD038465 by Portail BibCNRS INSU, Wiley Online Library on [09/01/2025]. See the Terms and Conditions (https://onlinelibrary.wiley.com/terms-and-conditions) on Wiley Online Library for rules of use; OA articles are governed by the applicable Creative Commons License

2.2.3. Validation Data

The Terra Moderate Resolution Imaging Spectro-radiometer (MODIS) Land Surface Temperature product MOD11A2 Version 6 from 2001 to 2018 was used to evaluate the performance of the FLake model in simulating LSWT. RMSE, mean bias error (BIAS), and Pearson correlation coefficient (R) were adopted for the evaluation. The MOD11A2 product offers an 8-days average surface temperature, including daytime and nighttime surface temperatures, at a spatial resolution of 1 km. Each pixel value in the MOD11A2 product is the simple average of all the corresponding daily surface temperature pixels in the MOD11A1 product gathered over 8 days. The surface temperature is estimated using the generalized split-window algorithm, which effectively acquires the temperature over lake surface. The bias between MOD11A2 data and in situ observations was less than 1°C (Duan et al., 2019; Wan, 2014). We eliminated grids near the water-land boundary and calculated monthly lake-wide average temperature. We also used the product's quality flag to improve the validation accuracy. Specifically, we identified observations in a specific month for a given lake if the area of null grid cells for that lake exceeded 20% of its total area in at least two satellite transits within that month. This means that if a large portion of unreliable observations occur for more than 16 days within a specific month for a given lake, the data for that month are deemed unrepresentative and unsuitable for characterizing the actual water temperature. Lakes with "unrepresentative" data for, on average, more than 3 months during ice-free periods within a year were excluded from trend validations. However, for lakes that occasionally had "unrepresentative" data, we still included all their monthly data for trend validations.

We used the lake ice phenology data set developed by the National Tibetan Plateau Data Center (Qiu, 2019) to assess the lake ice phenology output from the FLake model. The data set was generated based on the inversion of passive microwave remote sensing measurements. It includes the freeze-up start date, freeze-up end date, break-up start date, and break-up end date for 200 ice-covered lakes in the Northern Hemisphere from 2002 to 2018. For some large lakes, such as Qinghai Lake, the phenological data is available for the longer period of 1978–2018.

2.3. Lake Model Description

LSWT in our study includes water surface temperature and ice surface temperature. When a lake is frozen, LSWT represents the ice surface temperature, not the temperature of the water beneath the ice. The one-dimensional thermodynamic lake model, FLake, was used here to simulate LSWTs for the selected 91 large lakes from 1979 to 2018. FLake is a two-layer integral or bulk freshwater model and utilizes the concept of self-similarity to parameterize the temperature-depth curve (Mironov, 2008; Mironov et al., 2010). It, therefore, requires fewer external parameters and achieves higher computational efficiency than multi-layered finite difference models when simulating multiple lakes at regional or global scales (Li et al., 2022; Woolway & Merchant, 2019). FLake vertically divides the lake water into two layers: the mixed layer and the thermocline layer. Water within the mixed layer is thoroughly mixed, and its temperature is homogeneous vertically. The temperature in the thermocline layer is parameterized using a self-similarity theory initially employed to describe temperature changes in the ocean thermocline layer (Kitaigorodsky & Miropolsky, 1970). This theory assumes that the thermocline thickness does not change the shape of the temperature profile.

In addition, lake-ice layer, snow layer, and thermally active upper layer of lake sediments are also considered in the FLake model. The concept of self-similarity theory is applied to these layers as well. The default water albedo in FLake is 0.07, while an empirical function of ice surface temperature calculates the ice albedo. The snow albedo is assumed to be equal to the ice albedo. Solar radiation penetrating lake water is parameterized using the Beer-Lambert decay law. The estimation of momentum flux, latent heat flux, and sensible heat flux relies on the Monin-Obukhov similarity theory. The roughness lengths over the water or ice/snow surface are calculated comprehensively by considering wind speed, potential temperature, and air humidity (Zilitinkevich et al., 2001).

Meteorological variables driving FLake include air temperature, wind speed, downward shortwave radiation (SW), downward longwave radiation (LW), specific humidity, and surface pressure. Simulating individual lakes requires lake-specific parameters such as lake depth, albedo, light extinction coefficient, and fetch. The prognostic variables for model initialization include mixed layer temperature, mixed layer depth, bottom layer temperature, mean water column temperature, ice surface temperature, ice thickness, etc. To minimize the influence of the initial physical field on lake simulations, a spin-up process is usually necessary to reach an equilibrium state and

21698996, 2023, 21, Downloaded from https://agupubs.onlinelibrary.wiley.com/doi/10.1029/2022JD038465 by Portail BibCNRS INSU, Wiley Online Library on [09/01/2025]. See the Terms and Conditions (https://onlinelibrary.wiley.com/terms-and-conditions) on Wiley Online Library for rules of use; OA articles are governed by the applicable Creative Commons License

Table 1
Simulation Protocol for Quantifying the Respective Contribution of Air Temperature (Tair), Downward Longwave Radiation (LW), Wind Speed (Wind), Specific Humidity (Qair), and Downward Shortwave Radiation (SW) to the Trend in LSWT

Simulation ID	Tair	LW	Wind	Qair	SW
Exp1	1979–2018	1979–2018	1979–2018	1979–2018	1979–2018
Exp2	detrend	1979–2018	1979–2018	1979–2018	1979–2018
Exp3	1979–2018	detrend	1979–2018	1979–2018	1979–2018
Exp4	1979–2018	1979–2018	detrend	1979–2018	1979–2018
Exp5	1979–2018	1979–2018	1979–2018	detrend	1979–2018
Exp6	1979–2018	1979–2018	1979–2018	1979–2018	detrend

mimic the actual system. However, due to the absence of hypolimnion parameterization representation, FLake is unsuitable for simulating deep lakes' temperature profiles. Consequently, we implemented an "artificial depth" to limit the lake depth to a maximum of 60 m in the simulation (Martynov et al., 2010; Perroud et al., 2009). Given that only two of the lakes in the study have depths exceeding 60 m, the "artificial depth" limitation should not have too much impact on our simulation.

2.4. Simulation Protocol

To calculate the respective contributions of atmospheric forcing variables to LSWT trends, six experiments with different climatic conditions were conducted with FLake (Table 1). Exp1 was a reference simulation for which FLake was driven by time-varying forcing data from 1979 to 2018. In the simulations Exp2-Exp6, the investigated forcing variable was detrended while allowing all other variables to vary from 1979 to 2018. To detrend the forcing variables, we employed a method that involved removing the monthly trends of each variable while keeping the variable values unchanged for the initial year and subtracting the monthly trends from the subsequent years. The difference in the trends in LSWT between Exp1 and Exp2-Exp6 represented the contribution of the investigated variable in the Exp2-Exp6 simulations. The largest contributor to LSWT change at the lake or regional scales can be determined based on the contribution values of individual forcing variables.

Additionally, we devised two supplementary experiments to explore the potential impact of antecedent climatic conditions on LSWT changes. All atmospheric forcing variables are detrended for the period January–May in Exp S1 while detrended for the period June–August in Exp S2. Technically, for instance, in Exp S1, we removed the trends of all forcing variables, specifically from January to May, while keeping the trends intact from June to December. These additional experiments provide further insights into the factors influencing lake surface warming.

2.5. Trend Analysis

The Theil-Sen method was used to calculate the trends in LSWTs and climate variables. The significance of the trend was assessed using a nonparametric Mann-Kendall test at the 95% significance level. We validated the trends in simulated LSWTs with satellite data using different monthly averages over the period 2001–2018. In the first approach, we extracted the model output linearly at the times of satellite observations, specifically at 10:30 a.m. and 10:30 p.m., and averaged the output over an 8-days period. The 8-days output and satellite-derived LSWTs were then aggregated to calculate the monthly average using a time-weighted method. The time weighting is included to account for the shorter than 8-days periods at the beginning and end of each month. In the second approach, we calculated the monthly simulated LSWT by averaging the complete 3-hourly simulated output. Displaying trends in LSWT from 1979 to 2018, we used the monthly LSWT output calculated from the complete simulation. Additionally, based on lake area weighting, we calculated the dynamic changes in both national and sub-regional mean lake water temperature from 1979 to 2018.

3. Results

3.1. Validations Against Satellite Observations

We compared monthly simulated LSWT with satellite-derived LSWT for each of the six sub-regions over the period 2001–2018 when both data sources are available (Figure 2a). The magnitude of modeled LSWT agreed

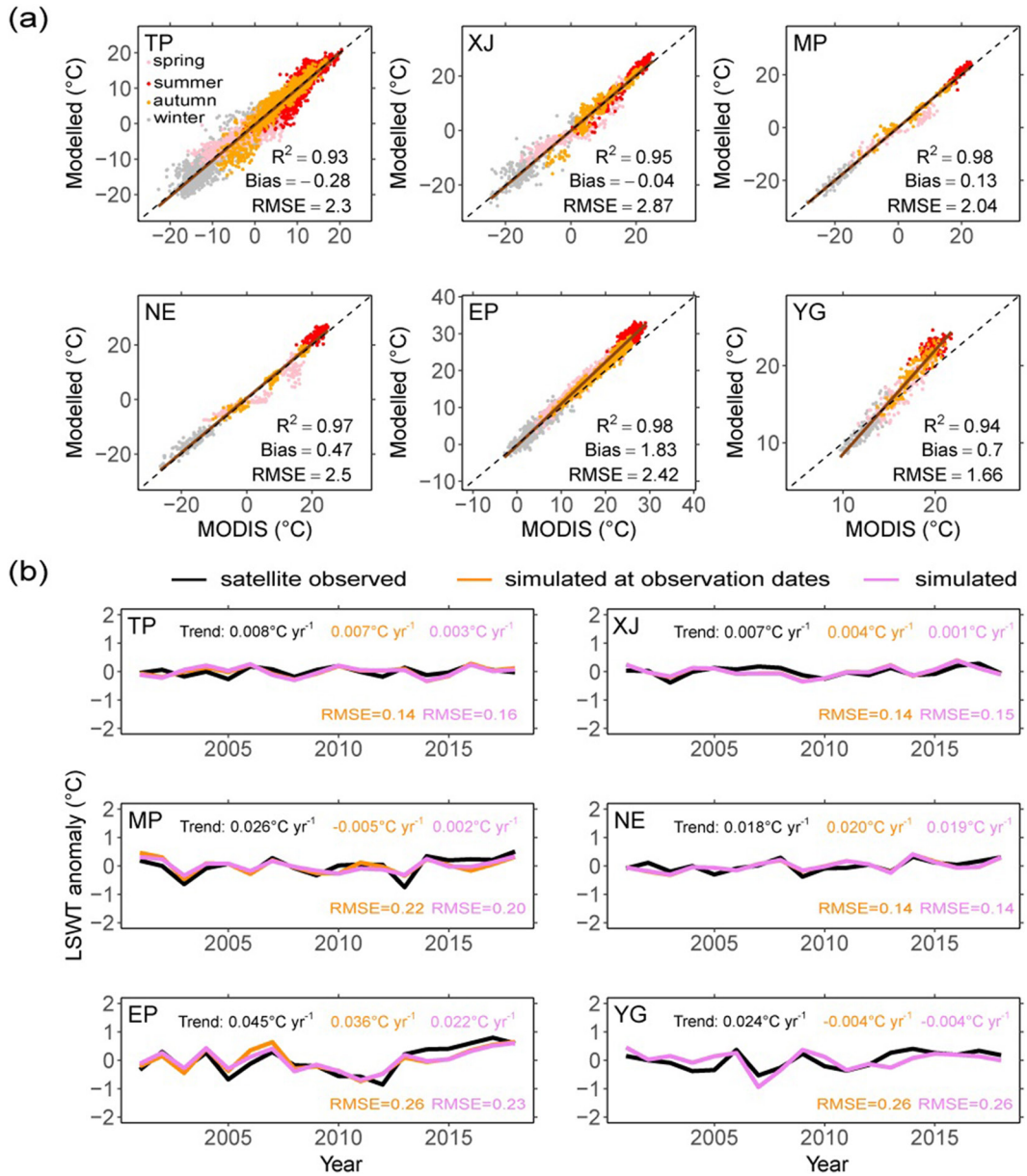

Figure 2. Validations of modeled lake surface water temperature (LSWT) against satellite-derived LSWT. (a) Comparisons between monthly modeled and observed LSWT in six sub-regions. The solid brown and dashed black lines represent the linear regression line and the 1:1 line, respectively. (b) Simulated and satellite-derived annual LSWT anomalies during the ice-free period for six sub-regions from 2001 to 2018. The black line represents the satellite observed LSWT. The orange line shows the simulated LSWT sampled at the times of satellite transit. The purple line represents the complete model results. Trends in the LSWT time series are indicated by the corresponding colors. TP: Tibetan Plateau; XJ: Xinjiang; MP: Inner-Mongolia Plateau; NE: Northeast Plain and Mountain; EP: Eastern Plain; YG: Yunnan-Guizhou Plateau.

well with that of MODIS LSWT in all the sub-regions (R^2's > 0.93). The FLake model also produces reasonable simulated LSWTs for six lakes by using lake-specific parameters from nearby lakes as inputs ($R^2 = 0.97$, Figure S1 in Supporting Information S1). However, the simulations using optimized lake-specific parameters based on the ARC-Lake data set slightly overestimated the LSWT in the EP and YG. This may be attributable to the cold bias in MODIS data (Wilson et al., 2013; Zhao et al., 2020) and the systematic deviation between the ARC-Lake and MODIS sensors (Wan et al., 2017), especially in the EP and YG (Figures S2 and S3 in Supporting Information S1). Even though the simulations slightly deviate from the MODIS data, the deviation does not affect the inter-annual variability and long-term trend of simulated LSWT.

21698996, 2023, 21, Downloaded from https://agupubs.onlinelibrary.wiley.com/doi/10.1029/2022JD038465 by Portail BibCNRS INSU, Wiley Online Library on [09/01/2025]. See the Terms and Conditions (https://onlinelibrary.wiley.com/terms-and-conditions) on Wiley Online Library for rules of use; OA articles are governed by the applicable Creative Commons License

21698996, 2023, 21, Downloaded from https://agupubs.onlinelibrary.wiley.com/doi/10.1029/2022JD038465 by Portail BibCNRS INSU, Wiley Online Library on [09/01/2025]. See the Terms and Conditions (https://onlinelibrary.wiley.com/terms-and-conditions) on Wiley Online Library for rules of use; OA articles are governed by the applicable Creative Commons License

Satellite-derived LSWTs are relatively sparse during the ice-covered period due to the mis-discrimination between clouds and lake ice or snow (Lazhu et al., 2016). Hence, we compared the inter-annual variation and long-term trend of modeled LSWT with satellite observation during the ice-free period from 2001 to 2018. FLake generally captured the inter-annual variability of satellite-derived LSWT (R^2's, 0.33–0.71, Figure 2b). The RMSEs range from 0.14 to 0.26°C when comparing the simulated and MODIS inter-annual LSWT anomalies. The trends from sampled simulations during satellite observations demonstrated greater consistency with satellite observations than trends derived from the entire simulation output (Figure 2b). Considering the sensitivity of the trend to minor errors over a relatively short 18-years period, the satellite-derived and simulated trends exhibit good agreement. However, the FLake model does not closely capture the trends of LSWTs as observed by satellite in the MP and YG. The FLake model underestimates the trends in LSWT in the MP, likely due to its neglect of the impacts of human activities, such as irrigation and coal mining, on lake area and lake depth (Tao et al., 2015). MODIS observations in the YG during the rainy season are largely absent (Figure S4 in Supporting Information S1), limiting their ability to reflect the actual inter-annual changes in lake water temperature accurately. A good agreement between the simulation and observation in the YG during the dry season (Figure S5 in Supporting Information S1), underscores the FLake model's ability to replicate the water temperature dynamics in the YG. Furthermore, the FLake model shows high skill in reproducing the time series of monthly LSWT in all six sub-regions (Figure S6 in Supporting Information S1). The long-term trends of modeled LSWTs are generally consistent with those observed in MODIS for individual lakes (Figure S7 in Supporting Information S1).

Besides effectively simulating LSWT, the FLake model has an overall rather good performance in simulating lake ice phenology (Figure S8a in Supporting Information S1). At the individual lake scale, the FLake model performs better in estimating the break-up end date than the freeze-up start date (Figure S8b in Supporting Information S1). The RMSE (BIAS) of the freeze-up start date and break-up end date were 17.2 days (4.6 days) and 17.4 days (−6.0 days), respectively. Lakes located at high latitudes and high altitudes in China are generally ice-covered for at least 3 months (Kirillin et al., 2017), suggesting that the simulation bias is still within a reasonable range. In summary, the FLake model is reliable for simulating long-term changes in the surface temperature of large lakes in China.

3.2. Temporal Trends in LSWT

3.2.1. Decadal Trends in LSWT

Figure 3a shows the spatial pattern of the simulated LSWT changes for the 91 large lakes across China during 1979–2018. We found an overall significant increase in simulated LSWT of 0.040°C yr^{-1} ($p < 0.05$) in China. Furthermore, of the 91 lakes, about 83.5% show a significant warming trend (0.053°C yr^{-1}, $p < 0.05$), while seven lakes suggest a significant cooling trend (−0.064°C yr^{-1}, $p < 0.05$). The remaining eight lakes do not show a statistically significant trend in LSWT (0.007°C yr^{-1}, $p > 0.05$). The trends in simulated LSWT range from −0.090 to 0.160°C yr^{-1}, implying a highly spatial heterogeneity of LSWT changes at a regional scale. This high spatial heterogeneity is especially clear in the TP, where lakes with the fastest warming and cooling rates are found. Significant increases in simulated LSWT are mainly found in the southern TP, southern EP, and northern XJ. In contrast, lakes in the eastern MP and the YG show relatively small simulated LSWT increases. Note that the decrease in simulated LSWT mainly occurred in the northwest of TP, which was also reported by Wan et al. (2018). The regional average LSWTs increase significantly in all six sub-regions (Figures 3b–3g), with the highest warming rate in the EP (0.049°C yr^{-1}) and the lowest in the YG (0.016°C yr^{-1}).

Annual simulated LSWT is warming at a rate of 0.040°C yr^{-1} at the national scale, while air temperature rises at a slightly higher rate (0.047°C yr^{-1}). Hence, at the national scale, the rate of increase of simulated LSWT is 85.7% of that of air temperature. However, 38 lakes out of the studied lakes located in the TP, XJ, NE, and EP displayed a warming rate faster than the air temperature (above 1:1 line; Figure 4). The TP, XJ, and NE lakes freeze for several months yearly, known as seasonally ice-covered lakes. Three lakes in the northern region of EP also experience seasonal ice cover. Other lakes in the EP occasionally freeze during cold winters but remain ice-free during warmer ones. Our simulations show that the increasing trend of surface water temperature exceeding air temperature occurred in seasonally ice-covered lakes and occasionally ice-covered lakes.

3.2.2. Seasonal Trends in LSWT

For different seasons, the simulations show that at the national scale, LSWT in winter increases the fastest (0.050°C yr^{-1}), followed by LSWT in spring (0.041°C yr^{-1}) and autumn (0.038°C yr^{-1}). LSWT in summer has

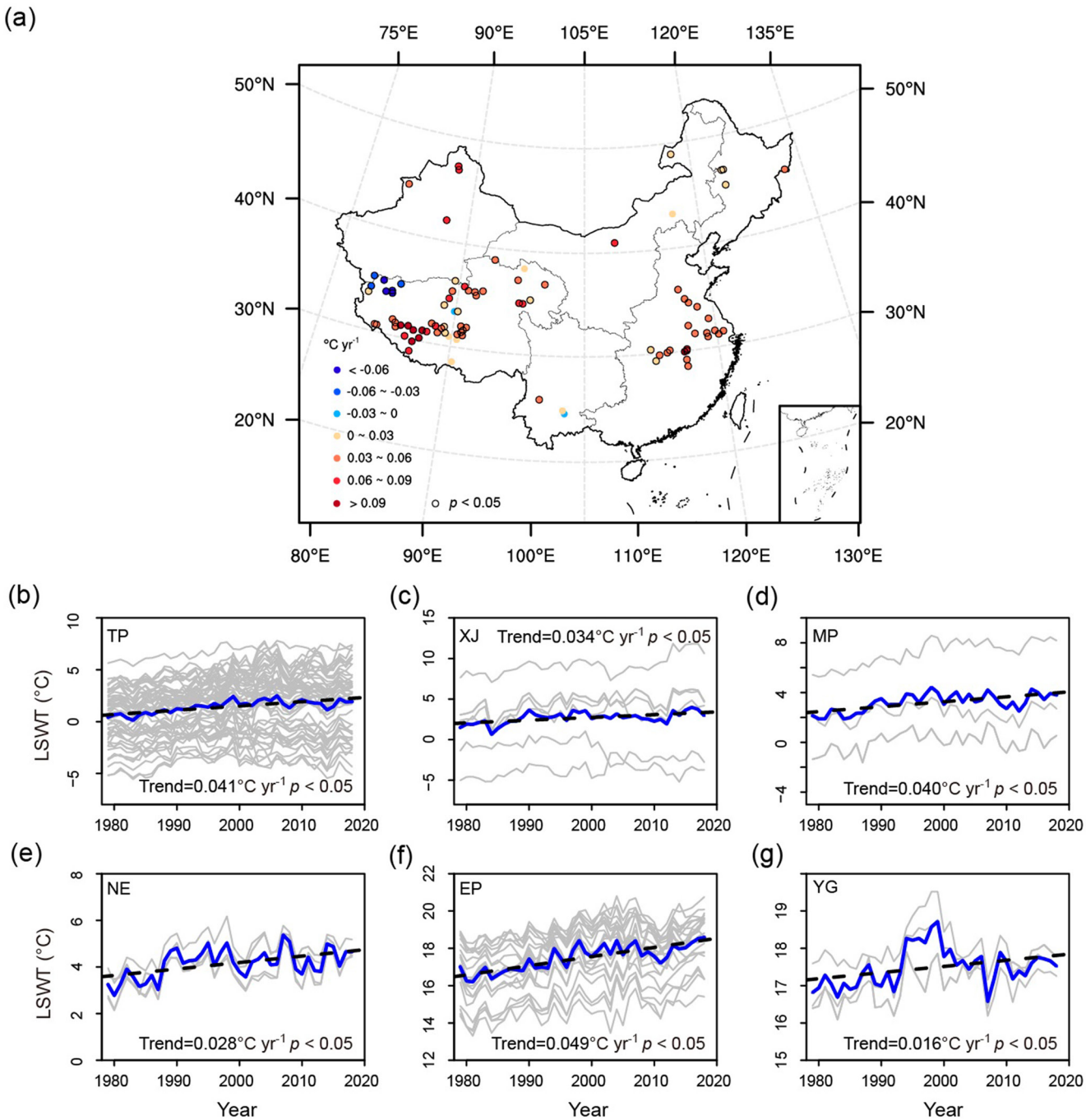

Figure 3. Trends in annual simulated lake surface water temperature (LSWT) for individual lakes (a) and sub-regions (b–g) over the period 1979–2018, respectively. Circles with black boundary lines in (a) indicate lakes with significant changes in LSWT ($p < 0.05$). The inset map in (a) shows the Nanhai Zhudao. The gray lines show the annual LSWTs for individual lakes (b–g). Blue and dashed black lines in (b)–(g) represent the average regional LSWT and its linear trend. TP: Tibetan Plateau; XJ: Xinjiang; MP: Inner-Mongolia Plateau; NE: Northeast Plain and Mountain; EP: Eastern Plain; YG: Yunnan-Guizhou Plateau.

the lowest increasing rate (0.029°C yr^{-1}). The LSWT warming rate in winter was almost twice that in summer. Apart from the overall seasonal pattern of modeled LSWT increase at the country scale, the season with the highest LSWT increase rate varies among the sub-regions (Figure 5). Regarding median values, lakes in the TP, XJ, and YG experience the most rapid increase in simulated LSWT during winter, while lakes in the MP and EP show the fastest increase in simulated LSWT during spring. The simulated lake water in the NE warms fastest in autumn. Relative to the overall significant rise of LSWT for each season, the increase of simulated

21698996, 2023, 21, Downloaded from https://agupubs.onlinelibrary.wiley.com/doi/10.1029/2022JD038465 by Portail BibCNRS INSU, Wiley Online Library on [09/01/2025]. See the Terms and Conditions (https://onlinelibrary.wiley.com/terms-and-conditions) on Wiley Online Library for rules of use; OA articles are governed by the applicable Creative Commons License

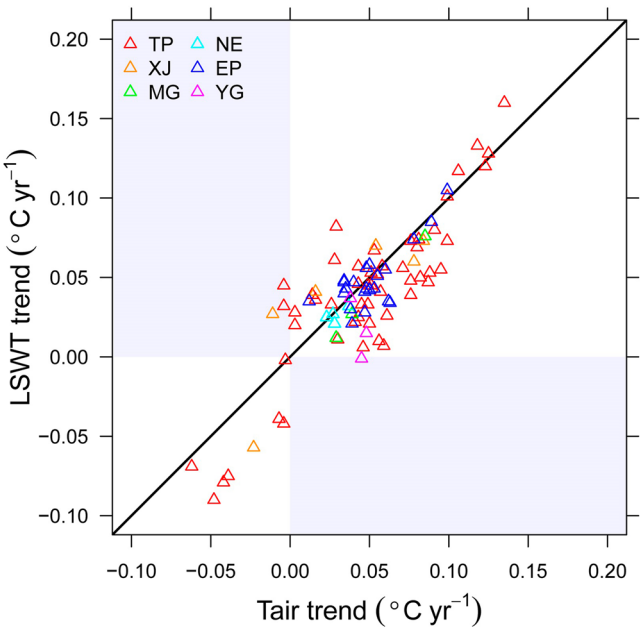

Figure 4. Scatterplot of simulated lake surface water temperature trends and air temperature (Tair) trends for the 91 large lakes in China. The black line is a 1:1 line. TP: Tibetan Plateau; XJ: Xinjiang; MP: Inner-Mongolia Plateau; NE: Northeast Plain and Mountain; EP: Eastern Plain; YG: Yunnan-Guizhou Plateau.

LSWT in spring (0.015°C yr^{-1}) and especially in winter (0.007°C yr^{-1}) is low in the NE. Lakes in the YG do not show significant changes in simulated LSWT in summer (0.003°C yr^{-1}) and autumn (0.007°C yr^{-1}). The trends of estimated LSWT for ice-covered lakes in winter and spring are likely influenced by the phase transition of water and ice, as well as the freezing and melting process of lake ice, which can significantly affect the water and heat exchange between the lake and the atmosphere.

3.3. Drivers of Temporal Trends in LSWT

With the six simulations implemented to separate and quantify individual climate forcing variables' contributions to the simulated LSWT trends from 1979 to 2018, we found that air temperature and wind speed are the largest climatic contributors to LSWT trends in 50 and 25 lakes, respectively (Figure 6a). Downward LW, downward SW, and specific humidity dominate LSWT variations for only 17.6% of the investigated lakes, mainly in the EP, XJ, and NE. On a national scale, air temperature, downward LW, wind speed, and specific humidity contribute 0.018°C yr^{-1} (45.0%), 0.014°C yr^{-1} (34.4%), 0.006°C yr^{-1} (14.4%), and 0.008°C yr^{-1} (20.0%) to the simulated LSWT rise, respectively. The contribution of downward SW to LSWT change is negative (−0.004°C yr^{-1} or −11.1%).

At the sub-region level, the simulations also suggest that air temperature, wind speed, and downward LW mainly drive the LSWT changes (Figure 6b). However, although all sub-regions show a significant increase in modeled LSWT, air temperature, downward LW, and specific humidity contribute

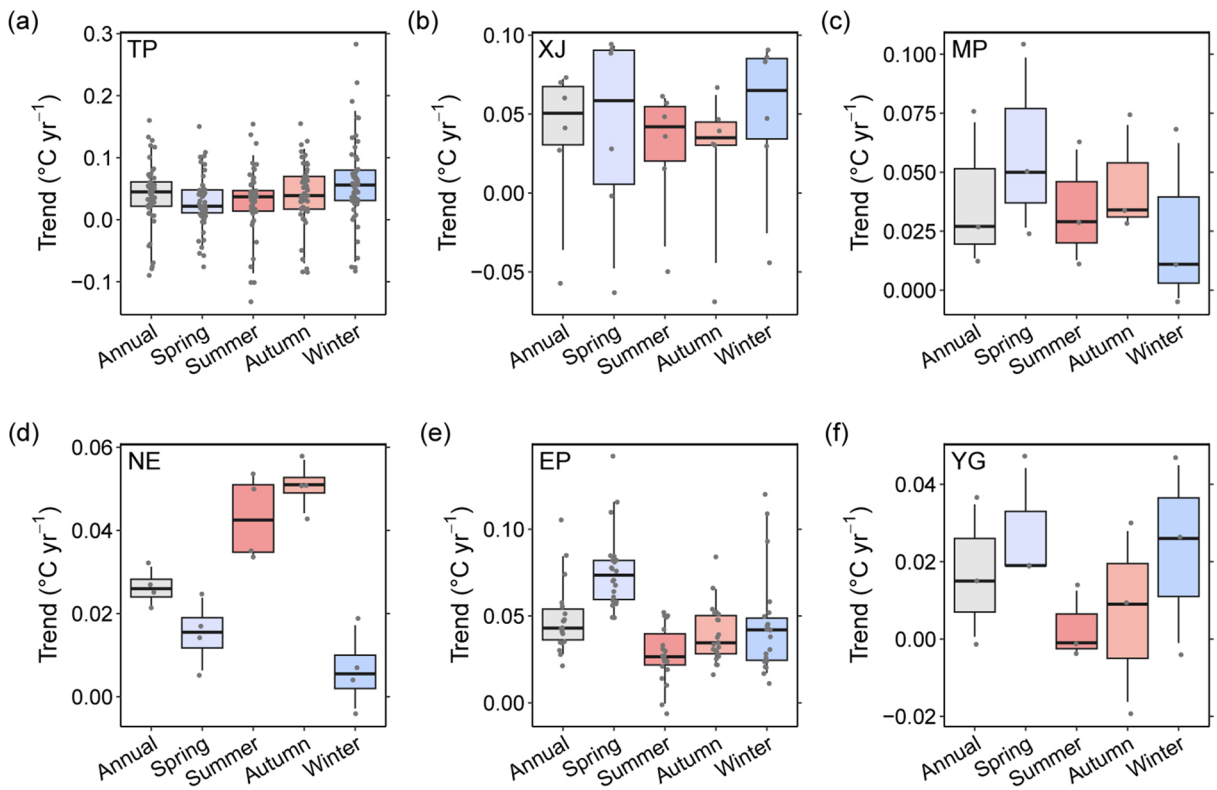

Figure 5. The simulated annual and seasonal lake surface water temperature (LSWT) trends in six sub-regions from 1979 to 2018. The boxes and whiskers present the 5th, 25th, 50th, 75th, and 95th percentiles of the LSWT trends. The gray dots represent the trends in LSWT for individual lakes. TP: Tibetan Plateau; XJ: Xinjiang; MP: Inner-Mongolia Plateau; NE: Northeast Plain and Mountain; EP: Eastern Plain; YG: Yunnan-Guizhou Plateau.

21698996, 2023, 21, Downloaded from https://agupubs.onlinelibrary.wiley.com/doi/10.1029/2022JD038465 by Portail BibCNRS INSU, Wiley Online Library on [09/01/2025]. See the Terms and Conditions (https://onlinelibrary.wiley.com/terms-and-conditions) on Wiley Online Library for rules of use; OA articles are governed by the applicable Creative Commons License

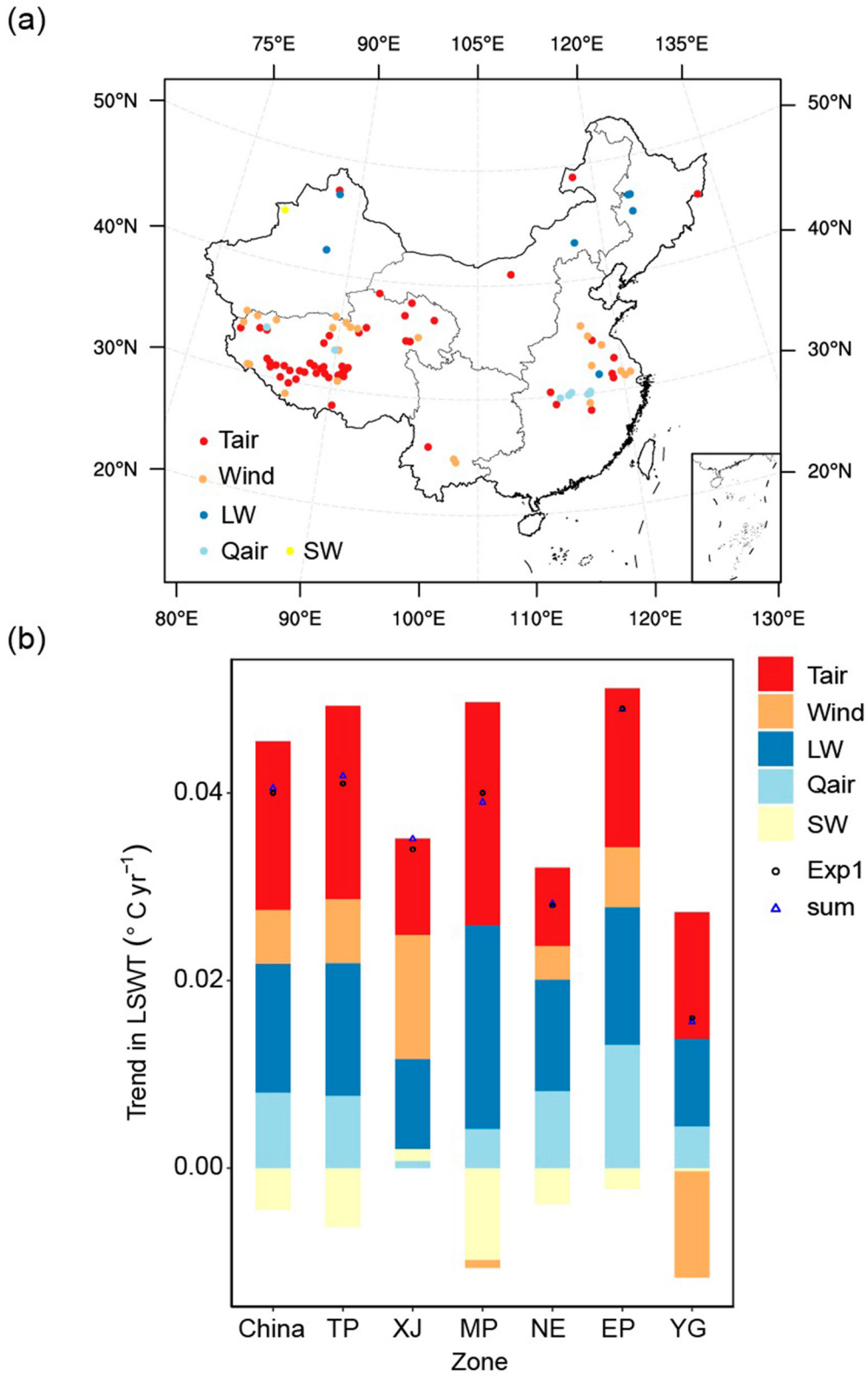

Figure 6.

21698996, 2023, 21, Downloaded from https://agupubs.onlinelibrary.wiley.com/doi/10.1029/2022JD038465 by Portail BibCNRS INSU, Wiley Online Library on [09/01/2025]. See the Terms and Conditions (https://onlinelibrary.wiley.com/terms-and-conditions) on Wiley Online Library for rules of use; OA articles are governed by the applicable Creative Commons License

21698996, 2023, 21, Downloaded from https://agupubs.onlinelibrary.wiley.com/doi/10.1029/2022JD038465 by Portail BibCNRS INSU, Wiley Online Library on [09/01/2025]. See the Terms and Conditions (https://onlinelibrary.wiley.com/terms-and-conditions) on Wiley Online Library for rules of use; OA articles are governed by the applicable Creative Commons License

nearly equally to the LSWT changes in NE, while the rising air temperature dominates the increases in LSWTs in the TP, MP, EP, and YG regions. More specifically, air temperature could account for 29.9%–50.4% changes in modeled LSWT in TP, XJ, NE, and EP, 59.6% in MP, and 84.5% in YG (Table S1 in Supporting Information S1). Furthermore, despite the air temperature being the primary driver of LSWT change in the YG, the increase in LSWT caused by air temperature (0.014°C yr^{-1}) was partly offset by a decrease in LSWT introduced by increasing wind speed (−0.011°C yr^{-1}). This led to the slowest estimated LSWT increase in the YG compared to other sub-regions. The significant decrease in estimated LSWT in the northwestern TP is associated with a decline in air temperature, downward LW, and an increase in wind speed (Figure S9 in Supporting Information S1). Approximately 45.2% of the decreased LSWT in these lakes can be attributable to wind speed. Air temperature, downward LW, and specific humidity are estimated to account for 15.8%–24.3% of the decrease in LSWT, whereas the contribution of downward SW is negligible (1.7%). The sum of individual contributions of each forcing variable is not equal to 100% (see circle and triangle in Figure 6b), indicating the role of inter-variable interactions (Li et al., 2019; Shi et al., 2022). Nevertheless, considering the relatively small gap between the sum of individual contributions and the LSWT trend under the Exp1 simulations, our attribution analysis of the LSWT trends is reliable in explaining the dominant drivers of lake warming across China. In addition, air temperature, downward LW, and wind speed are also the dominant factors driving the changes in estimated LSWT for all four seasons (Table S2 in Supporting Information S1).

4. Discussion

4.1. Spatial Heterogeneity of Temporal Trends

Over the past 40 years, our simulations show that the LSWTs of large Chinese lakes have increased by 1.61°C on average, at a mean rate of 0.040°C yr^{-1}. The average LSWT increase rate is comparable to a global scale study (O'Reilly et al., 2015), which reported a global average summer warming rate in LSWT of 0.034°C yr^{-1} over 235 large lakes from 1985 to 2009. Our simulation of the averaged lake surface warming rate at 0.041°C yr^{-1} in TP is similar to the mean rate of 0.037°C yr^{-1} between 2001 and 2015 for lakes greater than 10 km^2 (Wan et al., 2018). The finding that estimated surface warming for lakes in EP is strongest in spring is also supported by Li et al. (2019), who suggested that spring is the fastest warming season for four shallow lakes in the Yangtze River Basin from 1979 to 2017. Moreover, water temperature under ice holds greater ecological significance for lake ecosystems than the ice surface temperature during ice-covered periods. Accordingly, we estimated LSWT trends for each sub-region from 1979 to 2018, adjusting LSWT values to 0°C when lakes are ice-covered. This approach generates trends similar to previous calculations including ice surface temperature in the EP and YG regions, while yielding LSWT trends from 0.018 to 0.026°C yr^{-1} in the TP, XJ, MP, and NE regions (Figure S10 in Supporting Information S1). These trends are relatively lower because, as per our definition, under-ice water temperature is assumed as 0°C during the period when the lake is ice-covered for each year, resulting in a less increase in average annual water temperature.

When other atmospheric variables hold constant, lakes would warm more slowly than air temperature due to the feedback of evaporative cooling (Lenters et al., 2005; Wang et al., 2018). Schmid et al. (2014) predicted that the ratio of the warming rate of equilibrium LSWT to that of air temperature is in the range of 70%–85%. However, of the 91 large lakes, 38 lakes show a faster simulated LSWT warming than the ambient air. Such excessive warming of lake surface water has also occurred at Lake Superior (Austin & Colman, 2007) and Lower Lake Zurich (Schmid & Köster, 2016). On the other hand, the increase in estimated LSWT in YG is only 38.9% of the air temperature rise, well below the predicted 70%–85% by Schmid et al. (2014). The complex and heterogeneous interactions between air temperature and LSWT require further investigation.

Dominant factors controlling LSWT changes, including air temperature, downward LW, and wind speed, have been reported previously (Li et al., 2019; Shi et al., 2022; Yang et al., 2020). Our simulations indicate that air temperature and downward LW are the two most dominant factors driving simulated surface warming in large Chinese lakes. Air temperature is the largest factor influencing simulated LSWT trends, accounting for

Figure 6. Attribution of annual simulated lake surface water temperature (LSWT) trends. (a) Spatial distribution of the largest contributor to LSWT changes for each of the 91 large lakes in China. (b) Relative contributions of climate variables to the trend in simulated LSWT at national and sub-region scales. The individual contribution of changes in air temperature (Tair), wind speed (Wind), downward longwave radiation, downward shortwave radiation, and specific humidity (Qair) to the trends in simulated LSWT were calculated based on the six simulation protocols. The circle and triangle represent the LSWT trend under the Exp1 simulation and the sum of contributions of individual atmospheric variables, respectively. The inset map in (a) shows the Nanhai Zhudao.

21698996, 2023, 21, Downloaded from https://agupubs.onlinelibrary.wiley.com/doi/10.1029/2022JD038465 by Portail BibCNRS INSU, Wiley Online Library on [09/01/2025]. See the Terms and Conditions (https://onlinelibrary.wiley.com/terms-and-conditions) on Wiley Online Library for rules of use; OA articles are governed by the applicable Creative Commons License

approximately 45.0% of water temperature trends at the national scale. When analyzing changes in lake surface temperature, Schmid et al. (2014) suggested that effects of downward LW and air temperature should not be treated separately. Changes in downward LW are mostly a result of variations in air temperature. Downward LW is normally parameterized as an emissivity multiplied by air temperature to the fourth power and by the Stefan-Boltzmann constant. Therefore, we quantified the portion of changes in downward LW influenced by rising air temperature (scaling downward LW by air temperature to the fourth power). In winter and spring, air temperature changes account for over 86.3% of the trends in downward LW, while in summer, they explain approximately 29.6% of the trends (Figure S11 in Supporting Information S1). Considering the changes in downward LW due to air temperature changes, we find that winter and spring air temperatures contribute to 87.8% of the trends in LSWT, while summer air temperatures explain 48.7% of the trends in LSWT. Crucially, regardless of whether we attribute the effect of downward LW on water temperature to air temperature, the conclusion that air temperature is the primary driver of lake surface warming remains unchanged.

Despite the widespread lake warming trends across China, the simulations show a decrease in LSWT in the northwestern TP. Such anomalies occur not only on the lake surface but also on the glacier surface. The latter is known as the Karakoram Anomaly (Gardelle et al., 2012; Hewitt, 2005). These anomalies are associated with snow-albedo feedback at a local scale (Guo et al., 2019) and atmospheric circulation variability at a large scale (Forsythe et al., 2017; Liu et al., 2018). We notice that the simulated LSWT trend in the YG (0.016°C yr^{-1}) is only 40.0% of the national average (0.040°C yr^{-1}). Previous research has reported a significant decrease in surface wind speed in most parts of China (Fu et al., 2011; Lin et al., 2013). However, wind speed in the YG has an increasing trend over the past decades (Shi et al., 2015). Increasing wind speed over lakes could intensify vertical lake mixing, bringing more heat to deep water while cooling surface temperature. For example, we found that the mixed layer depth in the Fuxian Lake (a lake in YG) simulated with variant wind speed in Exp1 could be 0.3 m deeper than that modeled with wind speeds detrended in Exp4. Besides, stronger wind speeds would increase the heat losses by evaporation and sensible heat flux, resulting in cooler surface temperatures (Desai et al., 2009). The negative effects of increasing wind speed offset the positive impacts of air temperature on LSWT, consequently leading to the weak estimated LSWT trend in YG.

While most previous research on LSWT changes focused primarily on the influences of simultaneous atmospheric factors, Austin and Colman (2007) suggested that winter and spring climates have strongly affected Lake Superior's summer water temperature. Here, we investigated the effects of previous winter-spring atmospheric conditions on summer water temperature in China. As shown in Figure 7, the increases in June–September LSWT in TP and XJ have been weakened due to the fixed antecedent climatic conditions. In contrast, the changes in summer LSWT in other sub-regions are less affected by winter-spring climatic conditions. Furthermore, after removing the trends of all forcing variables from June to August, simulated LSWT trends in the TP, XJ, and YG decreased in summer and partially decreased in autumn before recovering from October to November. As most lakes in these sub-regions are deep lakes, we suggest that changes in summer forcing variables have a lagging effect on subsequent autumn water temperature changes in deep lakes. Hence, our results highlight the importance of considering the impact of antecedent climate change on LSWT changes, particularly in TP and XJ.

4.2. Uncertainties

Although FLake can well capture the magnitude and spatiotemporal pattern of LSWT, there are still some uncertainties in estimating LSWT with this model. We note that for some lakes mainly located in the northern TP, the FLake model underestimates the LSWT trend compared to the MODIS product (Figure S7 in Supporting Information S1). The underestimation may be related to the large uncertainty in the forcing data, partly due to the harsh climate conditions and a limited number of meteorological stations in the northern TP (Shi et al., 2022). Larger disparities in long-term trends are also observed in the MP and YG from 2001 to 2018. While the FLake model underestimated the warming trend of LSWT in the MP, potentially influenced by human activities (Xu et al., 2022), this discrepancy does not prevent us from understanding how climate change could have affected LSWT given its wide application in exploring the mechanisms of LSWT changes and high performance in reproducing the magnitude and the inter-annual variations in LSWT (Figure 2). The deviation between observations and simulations in the YG may be related to the frequent absence of LSWT observations during rainy season (Figure S4 in Supporting Information S1). In future studies, it will be necessary to use more in situ data for model calibration and validation in the YG.

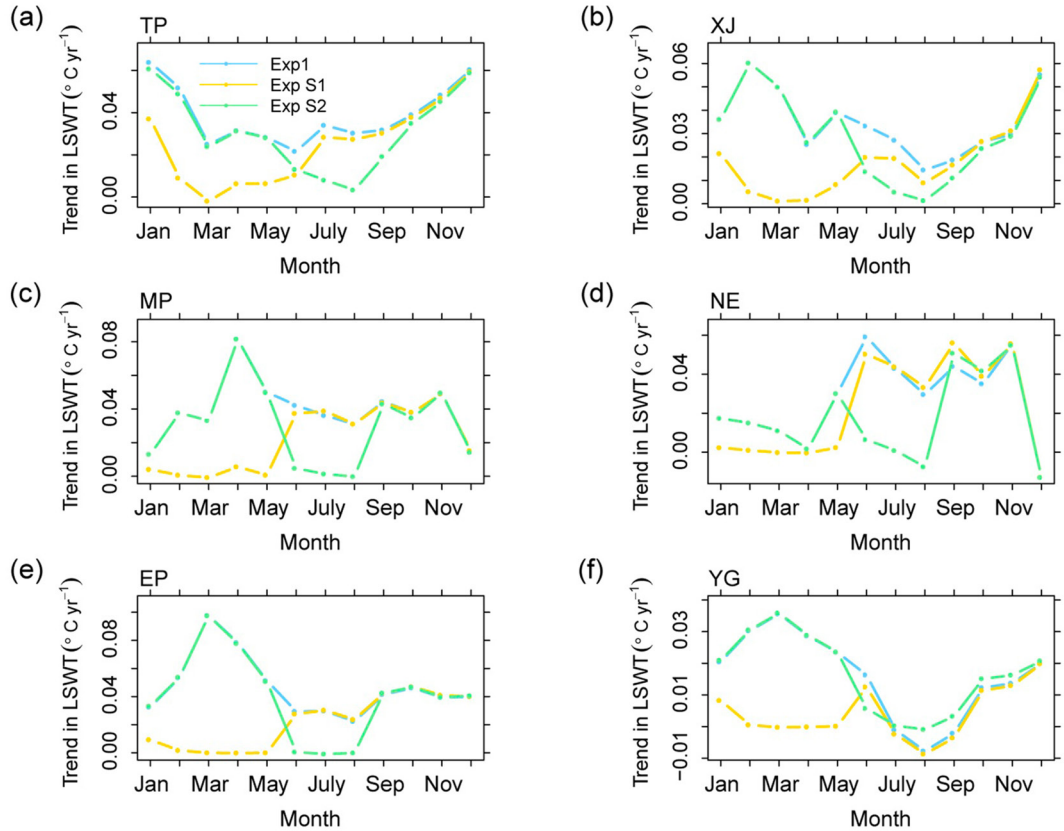

Figure 7. Monthly trends in lake surface water temperature in simulations assuming different antecedent and contemporary climatic conditions. Blue lines are the Exp1 simulations, with all forcing variables changing. Yellow lines represent the simulations of forcing variables that were detrended for January–May (Exp S1). Green lines represent the simulations of forcing variables that were detrended for June–August (Exp S2). TP: Tibetan Plateau; XJ: Xinjiang; MP: Inner-Mongolia Plateau; NE: Northeast Plain and Mountain; EP: Eastern Plain; YG: Yunnan-Guizhou Plateau.

With an offset of 1.62 m s^{-1}, the wind speed scaling formula removes all low wind speed events, introducing potential uncertainty into lake simulations. However, it does not affect the long-term trend of the simulated LSWT. Future studies using coupled lake-atmosphere models could aid in reducing the uncertainty. Inflows are essential in regulating the lake heat budget, especially for lakes downstream of rivers or glaciers. Zhang et al. (2014) suggested that glacier meltwater prevented the warming of glacial lakes. Neglecting meltwater inflow in the model may result in an overestimation of the LSWT trend in glacial lakes. Yang et al. (2020) pointed out that urban expansion and increased impervious surface increased runoff temperature into the lake. Urban expansion has been suggested to affect various atmospheric variables (Adamowski & Prokoph, 2013; Jauregui & Romales, 1996). However, its impact on LSWT changes in most large lakes is limited, except for small lakes near urban areas.

Lake depth and lake area were set to be constant in the FLake, without seasonal and inter-annual variations. These assumptions may have biased the seasonal and inter-annual variability of simulated LSWT. Additionally, the FLake model does not include ecological and geochemical processes within lakes. The variations in the light extinction coefficient caused by algae growth and the concentration of colored dissolved organic matter cannot be reflected in our simulations (Heiskanen et al., 2015; Paerl & Huisman, 2008). An in situ Secchi disk depth (SDD) data set of 170 Chinese lakes indicates that 130 of them experienced a significant decline in water clarity, with mean SDD falling from 1.89 m during the 1960s–1995 to 1.11 m during 2005–2016 (Zhang et al., 2020). The decline in water clarity may be responsible for underestimating simulated LSWT trends. FLake, as a one-dimensional lake model, excludes some processes, such as wind-driven circulation and lateral heat exchange (Aijaz et al., 2017; A. N. Huang et al., 2010). Three-dimensional (3-D) hydrodynamic models with highly spatially resolved and accurate meteorological forcing data might better characterize the thermal structure and circulation of large deep lakes (Song et al., 2004; Wu et al., 2021).

21698996, 2023, 21, Downloaded from https://agupubs.onlinelibrary.wiley.com/doi/10.1029/2022JD038465 by Portail BibCNRS INSU, Wiley Online Library on [09/01/2025]. See the Terms and Conditions (https://onlinelibrary.wiley.com/terms-and-conditions) on Wiley Online Library for rules of use; OA articles are governed by the applicable Creative Commons License

21698996, 2023, 21, Downloaded from https://agupubs.onlinelibrary.wiley.com/doi/10.1029/2022JD038465 by Portail BibCNRS INSU, Wiley Online Library on [09/01/2025]. See the Terms and Conditions (https://onlinelibrary.wiley.com/terms-and-conditions) on Wiley Online Library for rules of use; OA articles are governed by the applicable Creative Commons License

Small lakes, with an area of less than 100 km^2, account for 96% of the total number and 49% of the total area of Chinese lakes (Ma et al., 2011). However, due to the absence of accurate meteorological forcing data and lake-specific parameters, our study did not simulate or discuss the variations in water temperature in these lakes. Some extensive sub-regions, including the NE, MP, and YG, contain only a few unevenly distributed large lakes. The variations in LSWT of large lakes may not necessarily represent the LSWT variation characteristics of small lakes, as small lakes respond differently to climate change than larger lakes (Wang et al., 2019; Winslow et al., 2015). Larger lakes experience greater wind mixing due to increased surface momentum and exhibit greater variability in temperature and stratification variables than smaller lakes. Additionally, this variability increases with higher wind speeds (Magee & Wu, 2017).

4.3. Implications for Future Climate Change Effects on Lakes

Our simulations revealed that approximately 45.0% of the simulated surface warming in large Chinese lakes is caused by rising air temperatures. Rising downward LW and decreasing wind speed are the other two important causes. Global climate models project that air warming will continue over China, and wind speeds will decline in most parts of China (Wu et al., 2020; You et al., 2021). Thus, lake surface warming will likely be more severe, with important consequences for ecosystem functioning and services that warrant careful mitigation and management planning. Most lakes in China are in mesotrophic or eutrophic status (Le et al., 2010), and lake warming could stimulate the outbreak of cyanobacteria (Paerl & Paul, 2012; Rigosi et al., 2015). Fish assemblage composition, body size, and age structure would have changed due to water warming and eutrophication (Hansen et al., 2017; Jeppesen et al., 2012). Lakes in EP have historically supported productive fisheries, and changes in lake temperature would threaten fishery productivity and economic income. With the lake surface warming, the shortening of the ice-covered period for ice-covered lakes will lead to enhanced lake evaporation and lake-effect precipitation (Notaro et al., 2015). Lakes are one of the important sources of methane emissions (Crawford et al., 2014; Natchimuthu et al., 2016). Lake warming associated with increasing methane emissions would result in higher concentrations of greenhouse gases in the atmosphere, further accelerating global warming (Palma-Silva et al., 2013).

5. Conclusions

LSWT is sensitive to climate change, but its quantitative response to climate change remains uncertain. Using a one-dimensional thermodynamic lake model FLake, we analyzed the temporal and spatial variation of LSWT for 91 large lakes across China from 1979 to 2018 and quantified the relative contributions of atmospheric forcing variables to the LSWT trends. The model performs well in capturing satellite-derived LSWT changes, allowing us to use the model to simulate LSWT back to 1979 when MODIS LSWT products were unavailable. Our simulations show an overall lake surface warming trend in China with a mean rate of 0.040°C yr^{-1}. Approximately 83.5% of the simulated lake experienced a significant warming trend, while about 7.7% of the lakes, mainly distributed in the northwestern TP, exhibited significant cooling trends. Simulated LSWT trends show a high spatial heterogeneity, with the fastest warming rate in EP (0.049°C yr^{-1}) and the slowest in YG (0.016°C yr^{-1}). The simulated warming rates of LSWTs in spring and winter are more significant than those in summer and autumn. Meanwhile, our simulations show that 38 lakes (41.8%) warmed at a higher rate than the ambient air temperature. The attribution analysis shows that modeled lake surface warming is mainly caused by air temperature, downward LW, and wind speed. For individual lakes, the lakes with air temperature (wind speed) as the largest contributor to estimated LSWT trends account for 54.9% (27.5%) of the total investigated lakes. At the national scale, the air temperature is the largest driver of simulated rising LSWT (45.0%), followed by downward LW (34.4%), specific humidity (20.0%), wind speed (14.4%), and downward SW (−11.1%). Considering that the change in downward LW is primarily driven by higher air temperatures, rising air temperature continues to be the largest factor contributing to the warming of lake surfaces. By exploring the changes in LSWT and the contributions of atmospheric forcing variables to LSWT trends under global warming, this study helps deepen our understanding of how lake ecosystems respond to climate change.

Data Availability Statement

The HydroLAKES data set can be found at https://www.hydrosheds.org/products/hydrolakes (Messager et al., 2016). Salinity data of salty lakes can be accessed at http://yhzyhj.isl.ac.cn/page/list_hbls_dc.jsp (China Salty Lakes Resources and Environment Database, 2023). Lake-specific parameters, including lake depth, light

21698996, 2023, 21, Downloaded from https://agupubs.onlinelibrary.wiley.com/doi/10.1029/2022JD038465 by Portail BibCNRS INSU, Wiley Online Library on [09/01/2025]. See the Terms and Conditions (https://onlinelibrary.wiley.com/terms-and-conditions) on Wiley Online Library for rules of use; OA articles are governed by the applicable Creative Commons License

extinction coefficient, water albedo, white ice albedo, blue ice albedo, and fetch, are available at https://doi.org/10.1029/2021EA001737 (L. Huang et al., 2021). The China Meteorological Forcing Dataset is publicly available at https://data.tpdc.ac.cn/en/data/8028b944-daaa-4511-8769-965612652c49/ (He et al., 2020). The Moderate Resolution Imaging Spectroradiometer (MODIS/Terra) land surface temperature product (MOD11A2, v6) is obtained from https://lpdaac.usgs.gov/product_search/?query=MOD11%26view=cards%26sort=title (Wan, 2014). The lake ice phenology data set is developed by the National Tibetan Plateau Data Center and is obtained at http://data.tpdc.ac.cn/en/data/d4c69e7f-eb88-4555-845a-1638fd8ca9d3/ (Qiu, 2019). The source code and synopsis of routines for the FLake model can be accessed at http://www.flake.igb-berlin.de/ (Mironov, 2008). Figures in this manuscript were made by NCL version 6.6.2 (The NCAR Command Language, 2019) and R version 4.0.2 (R Core Team, 2021). The code for data processing and model output in this study are available in the repository "figshare" at https://doi.org/10.6084/m9.figshare.23736033.v2. The data supporting the findings of this study can also be acquired by contacting the corresponding author.

Acknowledgments

This study was supported by the National Key Research & Development Program of China (Grant 2019YFA0607302) and the Basic Science Center for Tibetan Plateau Earth System of National Natural Science Foundation of China (Grant 41988101). The authors sincerely appreciate the three anonymous reviewers for their insightful suggestions, which have greatly aided in improving the manuscript.

References

Adamowski, J., & Prokoph, A. (2013). Assessing the impacts of the urban heat island effect on streamflow patterns in Ottawa, Canada. *Journal of Hydrology*, *496*, 225–237. https://doi.org/10.1016/j.jhydrol.2013.05.032

Adrian, R., Reilly, C., Zagarese, H., Baines, S. B., Hessen, D. O., Keller, W., et al. (2009). Lakes as sentinels of climate change. *Limnology & Oceanography*, *54*(6), 2283–2297. https://doi.org/10.4319/lo.2009.54.6_part_2.2283

Aijaz, S., Ghantous, M., Babanin, A. V., Ginis, I., Thomas, B., & Wake, G. (2017). Nonbreaking wave-induced mixing in upper ocean during tropical cyclones using coupled hurricane-ocean-wave modeling. *Journal of Geophysical Research: Oceans*, *122*(5), 3939–3963. https://doi.org/10.1002/2016jc012219

Austin, J. A., & Colman, S. M. (2007). Lake Superior summer water temperatures are increasing more rapidly than regional air temperatures: A positive ice-albedo feedback. *Geophysical Research Letters*, *34*(6), L06604. https://doi.org/10.1029/2006gl029021

China Salty Lakes Resources and Environment Database. (2023). China salty lakes resources and environment database [Dataset]. Retrieved from http://yhzyhj.isl.ac.cn/page/list_hbls_dc.jsp

Crawford, J. T., Lottig, N. R., Stanley, E. H., Walker, J. F., Hanson, P. C., Finlay, J. C., et al. (2014). CO_2 and CH_4 emissions from streams in a lake-rich landscape: Patterns, controls, and regional significance. *Global Biogeochemical Cycles*, *28*(3), 197–210. https://doi.org/10.1002/2013gb004661

Desai, A. R., Austin, J. A., Bennington, V., & McKinley, G. A. (2009). Stronger winds over a large lake in response to weakening air-to-lake temperature gradient. *Nature Geoscience*, *2*(12), 855–858. https://doi.org/10.1038/ngeo693

Duan, S. B., Li, Z. L., Li, H., Göttsche, F. M., Wu, H., Zhao, W., et al. (2019). Validation of Collection 6 MODIS land surface temperature product using in situ measurements. *Remote Sensing of Environment*, *225*, 16–29. https://doi.org/10.1016/j.rse.2019.02.020

Forsythe, N., Fowler, H. J., Li, X. F., Blenkinsop, S., & Pritchard, D. (2017). Karakoram temperature and glacial melt driven by regional atmospheric circulation variability. *Nature Climate Change*, *7*(9), 664–670. https://doi.org/10.1038/nclimate3361

Fu, G. B., Yu, J. J., Zhang, Y. C., Hu, S., Ouyang, R., & Liu, W. (2011). Temporal variation of wind speed in China for 1961-2007. *Theoretical and Applied Climatology*, *104*(3–4), 313–324. https://doi.org/10.1007/s00704-010-0348-x

Gardelle, J., Berthier, E., & Arnaud, Y. (2012). Slight mass gain of Karakoram glaciers in the early twenty-first century. *Nature Geoscience*, *5*(5), 322–325. https://doi.org/10.1038/Ngeo1450

Guo, D., Sun, J., Yang, K., Pepin, N., Xu, Y., Xu, Z., et al. (2019). Satellite data reveal southwestern Tibetan Plateau cooling since 2001 due to snow-albedo feedback. *International Journal of Climatology*, *40*(3), 1644–1655. https://doi.org/10.1002/joc.6292

Guo, D., & Wang, H. (2013). Simulation of permafrost and seasonally frozen ground conditions on the Tibetan Plateau, 1981-2010. *Journal of Geophysical Research: Atmospheres*, *118*(11), 5216–5230. https://doi.org/10.1002/jgrd.50457

Hansen, G. J., Read, J. S., Hansen, J. F., & Winslow, L. A. (2017). Projected shifts in fish species dominance in Wisconsin lakes under climate change. *Global Change Biology*, *23*(4), 1463–1476. https://doi.org/10.1111/gcb.13462

He, J., Yang, K., Tang, W. J., Lu, H., Qin, J., Chen, Y., et al. (2020). The first high-resolution meteorological forcing dataset for land process studies over China [Dataset]. Scientific Data, *7*(1), 1–11. https://doi.org/10.1038/s41597-020-0369-y

Heiskanen, J. J., Mammarella, I., Ojala, A., Stepanenko, V., Erkkilä, K., Miettinen, H., et al. (2015). Effects of water clarity on lake stratification and lake-atmosphere heat exchange. *Journal of Geophysical Research: Atmospheres*, *120*(15), 7412–7428. https://doi.org/10.1002/2014jd022938

Hewitt, K. (2005). The Karakoram anomaly? Glacier expansion and the "elevation effect," Karakoram Himalaya. *Mountain Research and Development*, *25*(4), 332–340. https://doi.org/10.1659/0276-4741(2005)025[0332:Tkagea]2.0.Co;2

Hsu, S. A. (1988). *Coastal meteorology*. Academic Press Inc.

Huang, A. N., Lazhu, Wang, J. B., Dai, Y. J., Yang, K., Wei, N., et al. (2019). Evaluating and improving the performance of three 1-D lake models in a large deep lake of the central Tibetan Plateau. *Journal of Geophysical Research: Atmospheres*, *124*(6), 3143–3167. https://doi.org/10.1029/2018JD029610

Huang, A. N., Rao, Y. R., & Lu, Y. Y. (2010). Evaluation of a 3-D hydrodynamic model and atmospheric forecast forcing using observations in Lake Ontario. *Journal of Geophysical Research*, *115*(C2), C02004. https://doi.org/10.1029/2009jc005601

Huang, L., Wang, X. H., Sang, Y. X., Tang, S. C., Jin, L., Yang, H., et al. (2021). Optimizing lake surface water temperature simulations over large lakes in China with FLake model [Dataset]. Earth and Space Science, *8*(8). https://doi.org/10.1029/2021EA001737

Jauregui, E., & Romales, E. (1996). Urban effects on convective precipitation in Mexico City. *Atmospheric Environment*, *30*(20), 3383–3389. https://doi.org/10.1016/1352-2310(96)00041-6

Jeppesen, E., Mehner, T., Winfield, I. J., Kangur, K., Sarvala, J., Gerdeaux, D., et al. (2012). Impacts of climate warming on the long-term dynamics of key fish species in 24 European lakes. *Hydrobiologia*, *694*(1), 1–39. https://doi.org/10.1007/s10750-012-1182-1

Kirillin, G., Wen, L., & Shatwell, T. (2017). Seasonal thermal regime and climatic trends in lakes of the Tibetan highlands. *Hydrology and Earth System Sciences*, *21*(4), 1895–1909. https://doi.org/10.5194/hess-21-1895-2017

Kitaigorodsky, S., & Miropolsky, Y. Z. (1970). On the theory of the open ocean active layer. *Izvestiya—Atmospheric and Oceanic Physics*, *6*, 97–102.

Kraemer, B. M., Anneville, O., Chandra, S., Dix, M., Kuusisto, E., Livingstone, D. M., et al. (2015). Morphometry and average temperature affect lake stratification responses to climate change. *Geophysical Research Letters*, *42*(12), 4981–4988. https://doi.org/10.1002/2015gl064097
Layden, A., MacCallum, S. N., & Merchant, C. J. (2016). Determining lake surface water temperatures worldwide using a tuned one-dimensional lake model (FLake, v1). *Geoscientific Model Development*, *9*(6), 2167–2189. https://doi.org/10.5194/gmd-9-2167-2016
Lazhu, Yang, K., Wang, J. B., Lei, Y. B., Chen, Y. Y., Zhu, L. P., et al. (2016). Quantifying evaporation and its decadal change for Lake Nam Co, central Tibetan Plateau. *Journal of Geophysical Research: Atmospheres*, *121*(13), 7578–7591. https://doi.org/10.1002/2015JD024523
Le, C., Zha, Y., Li, Y., Sun, D., Lu, H., & Yin, B. (2010). Eutrophication of lake waters in China: Cost, causes, and control. *Environmental Management*, *45*(4), 662–668. https://doi.org/10.1007/s00267-010-9440-3
Lenters, J. D., Kratz, T. K., & Bowser, C. J. (2005). Effects of climate variability on lake evaporation: Results from a long-term energy budget study of Sparkling Lake, northern Wisconsin (USA). *Journal of Hydrology*, *308*(1–4), 168–195. https://doi.org/10.1016/j.jhydrol.2004.10.028
Li, X., Peng, S., Deng, X., Su, M., & Zeng, H. (2019). Attribution of lake warming in four shallow lakes in the middle and lower Yangtze River Basin. *Environmental Science & Technology*, *53*(21), 12548–12555. https://doi.org/10.1021/acs.est.9b03098
Li, X., Peng, S., Xi, Y., Woolway, R. I., & Liu, G. (2022). Earlier ice loss accelerates lake warming in the Northern Hemisphere. *Nature Communications*, *13*(1), 5156. https://doi.org/10.1038/s41467-022-32830-y
Lin, C. G., Yang, K., Qin, J., & Fu, R. (2013). Observed coherent trends of surface and upper-air wind speed over China since 1960. *Journal of Climate*, *26*(9), 2891–2903. https://doi.org/10.1175/Jcli-D-12-00093.1
Liu, Y., Chen, H., Wang, H., & Qiu, Y. (2018). The impact of the NAO on the delayed break-up date of lake ice over the southern Tibetan Plateau. *Journal of Climate*, *31*(22), 9073–9086. https://doi.org/10.1175/jcli-d-18-0197.1
Ma, R., Yang, G., Duan, H., Jiang, J., Wang, S., Feng, X., et al. (2011). China's lakes at present: Number, area and spatial distribution. *Science China Earth Sciences*, *54*(2), 283–289. https://doi.org/10.1007/s11430-010-4052-6
Magee, M. R., & Wu, C. H. (2017). Response of water temperatures and stratification to changing climate in three lakes with different morphometry. *Hydrology and Earth System Sciences*, *21*(12), 6253–6274. https://doi.org/10.5194/hess-21-6253-2017
Martynov, A., Sushama, L., & Laprise, R. (2010). Simulation of temperate freezing lakes by one-dimensional lake models: Performance assessment for interactive coupling with regional climate models. *Boreal Environment Research*, *15*(2), 143–164.
Messager, M. L., Lehner, B., Grill, G., Nedeva, I., & Schmitt, O. (2016). Estimating the volume and age of water stored in global lakes using a geo-statistical approach [Dataset]. Nature Communications, *7*(1), 13603. https://doi.org/10.1038/ncomms13603
Mironov, D. (2008). Parameterization of lakes in numerical weather prediction: Part 1. Description of a lake model. COSMO Technical Report No. 11. [Software]. http://www.cosmo-model.org
Mironov, D., Heise, E., Kourzeneva, E., Ritter, B., Schneider, N., & Terzhevik, A. (2010). Implementation of the lake parameterisation scheme FLake into the numerical weather prediction model COSMO. *Boreal Environment Research*, *15*(2), 218–230.
Natchimuthu, S., Sundgren, I., Galfalk, M., Klemedtsson, L., Crill, P., Danielsson, Å., et al. (2016). Spatio-temporal variability of lake CH_4 fluxes and its influence on annual whole lake emission estimates. *Limnology & Oceanography*, *61*(S1), S13–S26. https://doi.org/10.1002/lno.10222
Notaro, M., Bennington, V., & Vavrus, S. (2015). Dynamically downscaled projections of lake-effect snow in the Great Lakes Basin. *Journal of Climate*, *28*(4), 1661–1684. https://doi.org/10.1175/jcli-d-14-00467.1
O'Reilly, C. M., Alin, S. R., Plisnier, P. D., Cohen, A. S., & McKee, B. A. (2003). Climate change decreases aquatic ecosystem productivity of Lake Tanganyika, Africa. *Nature*, *424*(6950), 766–768. https://doi.org/10.1038/nature01833
O'Reilly, C. M., Sharma, S., Gray, D. K., Hampton, S. E., Read, J. S., Rowley, R. J., et al. (2015). Rapid and highly variable warming of lake surface waters around the globe. *Geophysical Research Letters*, *42*(24), 10773–10781. https://doi.org/10.1002/2015gl066235
Paerl, H. W., & Huisman, J. (2008). Climate—Blooms like it hot. *Science*, *320*(5872), 57–58. https://doi.org/10.1126/science.1155398
Paerl, H. W., & Paul, V. J. (2012). Climate change: Links to global expansion of harmful cyanobacteria. *Water Research*, *46*(5), 1349–1363. https://doi.org/10.1016/j.watres.2011.08.002
Palma-Silva, C., Marinho, C. C., Albertoni, E. F., Giacomini, I. B., Figueiredo Barros, M. P., Furlanetto, L. M., et al. (2013). Methane emissions in two small shallow neotropical lakes: The role of temperature and trophic level. *Atmospheric Environment*, *81*, 373–379. https://doi.org/10.1016/j.atmosenv.2013.09.029
Peng, X. Q., Frauenfeld, O. W., Jin, H. D., Du, R., Qiao, L. N., Zhao, Y. H., et al. (2021). Assessment of temperature changes on the Tibetan Plateau during 1980-2018. *Earth and Space Science*, *8*(4). https://doi.org/10.1029/2020EA001609
Perroud, M., Goyette, S., Martynov, A., Beniston, M., & Annevillec, O. (2009). Simulation of multiannual thermal profiles in deep Lake Geneva: A comparison of one-dimensional lake models. *Limnology & Oceanography*, *54*(5), 1574–1594. https://doi.org/10.4319/lo.2009.54.5.1574
Qiu, Y. (2019). The lake ice phenology dataset of the Northern Hemisphere (1978-2018) [Dataset]. National Tibetan Plateau/Third Pole Environment Data Center. https://doi.org/10.11888/Meteoro.tpdc.270981
R Core Team. (2021). R: A language and environment for statistical computing (version 4.0.2) [Software]. R Foundation for Statistical Computing. Retrieved from https://www.R-project.org/
Rigosi, A., Hanson, P., Hamilton, D. P., Hipsey, M., Rusak, J. A., Bois, J., et al. (2015). Determining the probability of cyanobacterial blooms: The application of Bayesian networks in multiple lake systems. *Ecological Applications*, *25*(1), 186–199. https://doi.org/10.1890/13-1677.1
Schmid, M., Hunziker, S., & Wuest, A. (2014). Lake surface temperatures in a changing climate: A global sensitivity analysis. *Climatic Change*, *124*(1–2), 301–315. https://doi.org/10.1007/s10584-014-1087-2
Schmid, M., & Köster, O. (2016). Excess warming of a Central European lake driven by solar brightening. *Water Resources Research*, *52*(10), 8103–8116. https://doi.org/10.1002/2016wr018651
Shi, P. J., Zhang, G. F., Kong, F., & Ye, Q. (2015). Wind speed change regionalization in China (1961–2012). *Advances in Climate Change Research*, *6*(2), 151–158. https://doi.org/10.1016/j.accre.2015.09.006
Shi, Y., Huang, A. N., Ma, W. Q., Wen, L., Zhu, L., Yang, X., et al. (2022). Drivers of warming in lake Nam Co on Tibetan Plateau over the past 40 years. *Journal of Geophysical Research: Atmospheres*, *127*(16), e2021JD036320. https://doi.org/10.1029/2021JD036320
Song, Y., Semazzi, F. H. M., Xie, L., & Ogallo, L. J. (2004). A coupled regional climate model for the Lake Victoria basin of East Africa. *International Journal of Climatology*, *24*(1), 57–75. https://doi.org/10.1002/joc.983
Steiner, A. L., Posselt, D. J., & Wright, D. M. (2013). Sensitivity of lake-effect snowfall to lake ice cover and temperature in the great lakes region. *Monthly Weather Review*, *141*(2), 670–689. https://doi.org/10.1175/mwr-d-12-00038.1
Su, D., Hu, X., Wen, L., Lyu, S., Gao, X., Zhao, L., et al. (2019). Numerical study on the response of the largest lake in China to climate change. *Hydrology and Earth System Sciences*, *23*(4), 2093–2109. https://doi.org/10.5194/hess-23-2093-2019
Tao, S., Fang, J., Ma, S., Cai, Q., Xiong, X., Tian, D., et al. (2019). Changes in China's lakes: Climate and human impacts. *National Science Review*, *7*(1), 132–140. https://doi.org/10.1093/nsr/nwz103
Tao, S., Fang, J., Zhao, X., Zhao, S., Shen, H., Hu, H., et al. (2015). Rapid loss of lakes on the Mongolian Plateau. *Proceedings of the National Academy of Sciences of the United States of America*, *112*(7), 2281–2286. https://doi.org/10.1073/pnas.1411748112

21698996, 2023, 21, Downloaded from https://agupubs.onlinelibrary.wiley.com/doi/10.1029/2022JD038465 by Portail BibCNRS INSU, Wiley Online Library on [09/01/2025]. See the Terms and Conditions (https://onlinelibrary.wiley.com/terms-and-conditions) on Wiley Online Library for rules of use; OA articles are governed by the applicable Creative Commons License

The NCAR Command Language. (2019). The NCAR command language (version 6.6.2) [Software]. UCAR/NCAR/CISL/TDD. https://doi.org/10.5065/D6WD3XH5

Wan, W., Li, H., Xie, H., Hong, Y., Long, D., Zhao, L., et al. (2017). A comprehensive data set of lake surface water temperature over the Tibetan Plateau derived from MODIS LST products 2001-2015. *Scientific Data*, *4*(1), 170095. https://doi.org/10.1038/sdata.2017.95

Wan, W., Zhao, L., Xie, H., Liu, B., Li, H., Cui, Y., et al. (2018). Lake surface water temperature change over the Tibetan Plateau from 2001 to 2015: A sensitive indicator of the warming climate. *Geophysical Research Letters*, *45*(20), 11177–11186. https://doi.org/10.1029/2018gl078601

Wan, Z. (2014). New refinements and validation of the collection-6 MODIS land-surface temperature/emissivity product [Dataset]. Remote Sensing of Environment, *140*, 36–45. https://doi.org/10.1016/j.rse.2013.08.027

Wang, B. B., Ma, Y. M., Wang, Y., Su, Z. B., & Ma, W. Q. (2019). Significant differences exist in lake-atmosphere interactions and the evaporation rates of high-elevation small and large lakes. *Journal of Hydrology*, *573*, 220–234. https://doi.org/10.1016/j.jhydrol.2019.03.066

Wang, W., Lee, X., Xiao, W., Liu, S., Schultz, N., Wang, Y., et al. (2018). Global lake evaporation accelerated by changes in surface energy allocation in a warmer climate. *Nature Geoscience*, *11*(6), 410–414. https://doi.org/10.1038/s41561-018-0114-8

Wilson, R. C., Hook, S. J., Schneider, P., & Schladow, S. G. (2013). Skin and bulk temperature difference at Lake Tahoe: A case study on lake skin effect. *Journal of Geophysical Research: Atmospheres*, *118*(18), 10332–310346. https://doi.org/10.1002/jgrd.50786

Winslow, L. A., Read, J. S., Hansen, G. J. A., & Hanson, P. C. (2015). Small lakes show muted climate change signal in deepwater temperatures. *Geophysical Research Letters*, *42*(2), 355–361. https://doi.org/10.1002/2014gl062325

Woolway, R. I., Dokulil, M. T., Marszelewski, W., Schmid, M., Bouffard, D., & Merchant, C. J. (2017). Warming of Central European lakes and their response to the 1980s climate regime shift. *Climatic Change*, *142*(3–4), 505–520. https://doi.org/10.1007/s10584-017-1966-4

Woolway, R. I., & Merchant, C. J. (2017). Amplified surface temperature response of cold, deep lakes to inter-annual air temperature variability. *Scientific Reports*, *7*(1), 4130. https://doi.org/10.1038/s41598-017-04058-0

Woolway, R. I., & Merchant, C. J. (2019). Worldwide alteration of lake mixing regimes in response to climate change. *Nature Geoscience*, *12*(4), 271–276. https://doi.org/10.1038/s41561-019-0322-x

Wu, J., Shi, Y., & Xu, Y. (2020). Evaluation and projection of surface wind speed over China based on CMIP6 GCMs. *Journal of Geophysical Research: Atmospheres*, *125*(22), e2020JD033611. https://doi.org/10.1029/2020JD033611

Wu, Y., Huang, A., Lu, Y., Lazhu, Yang, X., Qiu, B., et al. (2021). Numerical study of the thermal structure and circulation in a large and deep dimictic lake over Tibetan Plateau. *Journal of Geophysical Research: Oceans*, *126*(10), e2021JC017517. https://doi.org/10.1029/2021jc017517

Xu, Y., Gun, Z., Zhao, J., & Cheng, X. (2022). Variations in lake water storage over Inner Mongolia during recent three decades based on multi-mission satellites. *Journal of Hydrology*, *609*, 127719. https://doi.org/10.1016/j.jhydrol.2022.127719

Yang, J. X., Huang, M. T., & Zhai, P. M. (2021). Performance of the CRA-40/land, CMFD, and ERA-Interim datasets in reflecting changes in surface air temperature over the Tibetan Plateau. *Journal of Meteorological Research*, *35*(4), 663–672. https://doi.org/10.1007/s13351-021-0196-x

Yang, K., Yu, Z., & Luo, Y. (2020). Analysis on driving factors of lake surface water temperature for major lakes in Yunnan-Guizhou Plateau. *Water Research*, *184*, 116018. https://doi.org/10.1016/j.watres.2020.116018

Yang, K., Yu, Z., Luo, Y., Zhou, X., & Shang, C. (2019). Spatial-temporal variation of lake surface water temperature and its driving factors in Yunnan-Guizhou Plateau. *Water Resources Research*, *55*(6), 4688–4703. https://doi.org/10.1029/2019wr025316

You, Q. L., Cai, Z. Y., Wu, F. Y., Jiang, Z., Pepin, N., & Shen, S. S. P. (2021). Temperature dataset of CMIP6 models over China: Evaluation, trend and uncertainty. *Climate Dynamics*, *57*(1–2), 17–35. https://doi.org/10.1007/s00382-021-05691-2

Zhang, G., Yao, T., Xie, H., Qin, J., Ye, Q., Dai, Y., et al. (2014). Estimating surface temperature changes of lakes in the Tibetan Plateau using MODIS LST data. *Journal of Geophysical Research: Atmospheres*, *119*(14), 8552–8567. https://doi.org/10.1002/2014jd021615

Zhang, Y. L., Qin, B. Q., Shi, K., Zhang, Y. B., Deng, J. M., Wild, M., et al. (2020). Radiation dimming and decreasing water clarity fuel underwater darkening in lakes. *Science Bulletin*, *65*(19), 1675–1684. https://doi.org/10.1016/j.scib.2020.06.016

Zhao, G., Gao, H. L., & Cai, X. M. (2020). Estimating lake temperature profile and evaporation losses by leveraging MODIS LST data. *Remote Sensing of Environment*, *251*, 112104. https://doi.org/10.1016/j.rse.2020.112104

Zhong, Y. F., Notaro, M., Vavrus, S. J., & Foster, M. J. (2016). Recent accelerated warming of the Laurentian Great Lakes: Physical drivers. *Limnology & Oceanography*, *61*(5), 1762–1786. https://doi.org/10.1002/lno.10331

Zilitinkevich, S. S., Grachev, A. A., & Fairall, C. W. (2001). Scaling reasoning and field data on the sea surface roughness lengths for scalars. *Journal of the Atmospheric Sciences*, *58*(3), 320–325. https://doi.org/10.1175/1520-0469(2001)058<0320:Nacraf>2.0.Co;2

21698996, 2023, 21, Downloaded from https://agupubs.onlinelibrary.wiley.com/doi/10.1029/2022JD038465 by Portail BibCNRS INSU, Wiley Online Library on [09/01/2025]. See the Terms and Conditions (https://onlinelibrary.wiley.com/terms-and-conditions) on Wiley Online Library for rules of use; OA articles are governed by the applicable Creative Commons License